This is a private English translation by TH of the following article that has been published in
Bulletin of Volcanological Society of Japan, 64, 2, 103-119 (2019)
doi: 10.18940/kazan.64.2_103

On the Source Characteristics of Demagnetization and Ground Deformation Associated with Non-magmatic Activity

Takeshi HASHIMOTO[*], Mitsuru UTSUGI[**], Takahiro OHKURA[**],
Wataru KANDA[***], Akihiko TERADA[***], Satoshi MIURA[****]
and Masato IGUCHI[*****]

[*]Institute of Seismology and Volcanology, Faculty of Science, Hokkaido University, N10W8, Kita-ku, Sapporo, Hokkaido 060-0810, Japan.
[**]Aso Volcanological Laboratory, Institute for Geothermal Sciences, Sakanashi 3028, Aso, Kumamoto 869-2611, Japan.
[***]Volcanic Fluid Research Center, Tokyo Institute of Technology, Kusatsu 641-36, Kusatsu, Agatsuma, Gunma 377-1711, Japan.
[****]Research Center for Prediction of Earthquakes and Volcanic Eruptions, Graduate School of Science, Tohoku University, Aoba 6-6, Aramaki, Aoba-ku, Sendai, Miyagi 060-0810, Japan.
[*****]Sakurajima Volcano Research Center, Disaster Prevention Research Institute, Kyoto University, 1722-19, Sakurajima-Yokoyama, Kagoshima 891-1419, Japan.

Corresponding author: Takeshi Hashimoto
e-mail: hasimoto@sci.hokudai.ac.jp

Abstract

We collected information on non-magmatic unrest events reported mainly of Japanese volcanoes that have been monitored for extended time periods, with the aim of conducting a statistical evaluation of these phenomena, which can sometimes lead to an eruption. We assessed the geomagnetic field changes and ground deformation, which indicate demagnetization and inflation, respectively. We then compiled the source depth, intensity, and the rate (i.e., changes in magnetic moment or deformation volume per unit time), based on the single magnetic dipole model or the Mogi model, since these models are the most frequently cited in the literature. We found clear positive correlations between the source depth and its intensity and rate, exhibiting a linear trend on the log-log scatter plots. We confirmed that all the magnetic events and some of the deformation events were plotted markedly above the cutoff line related to the detection limit. We suspected that the geometry of the monitoring network and/or the simplistic point-source modeling could contribute to these positive correlations; otherwise some physical requirements such as subsurface structure might be the cause.

Although the number of unrest events collected was small, we investigated the validity of the evaluation of these unrest events from different viewpoints. Upward deviation from the linear trend on the scatter plot was found to be a potentially useful criterion, whereas the source depth had no definitive relationship with the subsequent occurrence of eruptions.

We assert that observable non-magmatic unrest events should be plotted within a diagonal area between the lower-right and upper-left domains in a scatter plot of source intensity (or rate) and depth. This is because weak sources at great depths cannot be detected, while overly strong sources close to the ground surface are physically impossible. In the intermediate zone, "unerupted" and "erupted" unrest events both occur. Based on this idea, we propose a statistical evaluation of the severity of unrest events, by measuring the deviation from the "unerupted unrests", although this hypothesis must be tested with a sufficient number of unrest events in the future. Meanwhile, care must be taken in interpreting the data collected here, since they are based on the simplified point-source models that assume a uniform half-space, and they may not accurately recreate the physical entities.

Further studies that can relate the physical conditions and their time evolution in the subsurface to geophysical monitoring records at the ground surface will be necessary to evaluate how such unrest events are related to eruptions.

Key words: non-magmatic unrest, phreatic eruption, demagnetization, Mogi source, statistical evaluation

1. Introduction

Phreatic eruptions are generally believed to be lack remarkable immediate precursors such as an acceleration of seismicity or ground deformation, and hence, their timing of initiation is relatively difficult to predict as compared to magmatic eruptions (Rouwet *et al.*, 2014; de Moor *et al.*, 2016). As indicated in the previous studies on phreatic eruptions and related eruptive phenomena (e.g., Mastin, 1991; Barberi *et al.*, 1992; Browne and Lawless, 2001; Rouwet and Morrissey, 2015), terminology related to phreatic eruptions is somewhat diverse and depends on the research field (Rouwet *et al*., 2014). In this study, besides strict definitions, we refer to the term phreatic eruption, in a broad sense, to indicate non-magmatic eruptions. Existence of ground water and/or a shallow hydrothermal system within a volcanic edifice is generally postulated, when we discuss phreatic eruptions and associated volcanic activities. Volcanoes that host a shallow hydrothermal system are often accompanied by persistent geothermal anomalies, steaming ground, hot springs, active crater lakes, and hydrothermal alterations. Many of them have quasi-steady microseismicity and/or sluggish ground deformation during inter-eruptive periods. In some cases, such background activity waxes and wanes in a timescale ranging from years to decades. Rouwet *et al*. (2014) called such anomalous waxing of inter-eruptive volcanic activities without evidence for "magma-on-the-move," as non-magmatic unrest. Although this phenomenon may reflect a certain change in the shallow hydrothermal system, it is currently difficult to link these events to the assessment of eruption imminence, or to the prediction of eruption intensity with a physical basis.

Meanwhile, some recent studies have indicated that an impermeable seal layer in a shallow hydrothermal system or conduit obstruction due to deposition of alteration minerals can be important factors in the processes leading to a phreatic/hydrothermal eruption (e.g., Christenson *et al*., 2010; Tanaka *et al*., 2017, 2018; Stix and de Moor, 2018). If this is the case, monitoring such processes can be a clue to better understanding the build-up phase of a phreatic eruption. In this study, we conducted a bibliographic survey of non-magmatic unrest events, mainly from Japanese volcanoes, that have been monitored for extended time periods. We discussed the collective characteristics of the modeled sources, focusing on the geomagnetic field changes and ground deformation. For comparison, we additionally include some specific events with magmatic influences in the course of an eruptive activity. In this study, we particularly note of the relationship between the depth and intensity (and its rate of change) of the modeled sources. As stated by Rouwet *et al*. (2014), the background activity level differs from volcano to volcano. Ideally, it is desirable to quantify the specific level of background activity for each volcano as accurately as possible in advance and identify the events that deviate from it as "unrest" to probabilistically evaluate its severity. Although such an approach may be possible in the future, it is presently unlikely to work well as data accumulation for individual volcanoes is still insufficient. In the current situation, we consider it is practically meaningful to handle the cases from multiple volcanoes collectively so that we find a common feature among individual volcanoes. Regarding the geomagnetic field changes (i.e., the so-called volcano-magnetic effect), it has been one of the basic volcano-monitoring items in Japan and several volcanoes have magnetic field records for decades. However, a geomagnetic observation aiming for volcano monitoring is quite unpopular in other countries, except for certain studies that have reported the short-period variations possibly due to the piezomagnetic effect (i.e., stress-induced response of rock’s magnetization) associated with a fissure eruption or an explosive eruption. Moreover, sluggish changes with a timescale ranging from years to decades have been hardly investigated. We considered that such records of unrest events at Japanese volcanoes are worth compiling and introducing worldwide.

2. Policy of compiling the unrest events

In modeling volcanic ground deformation, the Mogi model (spherical source model) is most frequently cited. For magnetic field changes, a single dipole model (mathematically equivalent to a uniformly magnetized spherical source) has most frequently been applied in the literature surveyed. In recent years, more sophisticated models that require an increased number of defining parameters have also been in use. However, such a source also requires the field data with sufficient spatial coverage, which are not always acquired in ordinary situations, especially in earlier studies. Thus, in this study, we collected and compiled the reported source models based on the Mogi model for deformation and the single dipole model for magnetism from the viewpoint of the case number. In particular, we dealt with relatively slow (with a duration of months to years) inflating deformations and demagnetizing events during inter-eruptive periods to pick up the source parameters such as depth, intensity (i.e., volumetric changes or magnetic moment changes), and its rate in time. We referred to the source parameters, if they are provided in the literature. For several events lacking the reported source models, we independently calculated them from the time-series records. Regarding the cases in which the source intensity was provided but not for the intensity rate, we calculated it by dividing the intensity with the duration of the relevant event. Note that some deformation events were accompanied by simultaneous demagnetization. However, the event name was given individually for demagnetization and deformation, as they were often separately reported in the literature (Tables 1 and 2). For readers’ information, we listed the events with both demagnetization and inflation as follows. [demagnetization: inflation], Tokachidake [Tk: Tk1/2], Tarumae [Tr: Tr1], Azuma [Az1: Az1/2/3], Adatara [Ad: Ad], Kusatsu-shirane [Ks3: Ks], Kuchinoerabujima [Kc3: Kc2]; [Kc4: Kc3]. Note that the duration used for modeling was not necessarily the same between deformation and magnetism.

We produced the scatter plots of the source intensity or its rate with respect to the source depth in the log-log scale shown in Figs. 1 to 4. We converted a source altitude into a depth from the ground surface, when necessary. Note that a source depth had a certain ambiguity if it was very shallow because the depth depended on where we took the ground level as the reference. We added error bars in the plots, if the estimation errors were provided in the literature.

3. Geomagnetic field changes

The so-called volcano-magnetic effects are the magnetic field changes associated with a volcanic activity. Among them, the thermomagnetic effect (i.e., changes in rock magnetization due to temperature) is considered a dominant mechanism explaining the magnetic field changes related to shallow volcanic processes with a timescale of days to years. Based on the thermomagnetic effect, magnetization of a rock decreases when it is heated (demagnetization), and vice versa (re-magnetization). In this study, we deal with demagnetization cases only, because we are focusing on an unrest process in which a temperature increase at a certain depth is envisaged. We briefly review each demagnetization event as follows. Note that the event names in the text (such as Mp1) are identical to those in Figs. 1 and 2 and Table 1, unless noted otherwise.

At Meakandake, Japan Meteorological Agency (JMA) has been monitoring the geomagnetic total field around the Ponmachineshiri crater since 1992. Takahashi *et al*. (2018) reported the demagnetization events observed in 2008–2009 (Mp1) and in 2013–2014 (Mp2). As for Mp1, a phreatic eruption occurred in November 2008. Note that most of the demagnetizing field changes of this event were achieved in the post-eruptive period, although the initiation preceded the eruption. This event was characterized by a relatively deep source with a large intensity (magnetic moment change) as compared to other events. In contrast, no eruption occurred around the event Mp2, which had a relatively shallow source. According to the time series plot of the continuous records in Takahashi *et al*. (2018), the events Mp1 and Mp2 showed a ramp-like change with the early and final phases having milder slopes than the middle. Thus, a simple division of the reported moment by the duration of changes underestimates the moment rate. Accordingly, we calculated the moment rate by using the central portion of the events, where the slope was mostly constant. Besides these two events at the Ponmachineshiri crater, Tanaka *et al*. (2016) reported a shallow demagnetization event (Mn) around the Nakamachineshiri crater based on their repeated surveys from 2014 to 2015.

At Tokachidake, Hokkaido University and the JMA started repeated surveys around the 1926 (Taisho cr.) and 1962 (62-I to III) craters in 2008. Hashimoto *et al*. (2010) reported a demagnetization event (Tk) sourced at a shallow depth just below the 62-II crater, based on the repeated surveys from 2008 to 2009. Since then, the demagnetizing trend has continued for ten years with some episodic accelerations, as well as a companion ground inflation localized to the crater (Regional Volcanic Observation and Warning Center, Sapporo Regional Headquarters, JMA, 2018).

At Mt. Tarumae, the JMA commenced repeated surveys in the summit atrio in 1999. Hokkaido University began collaborating with them to keep monitoring with an increased number of measurement sites (Meteorological Research Institute, 2008; Hashimoto *et al*., 2018). A demagnetization event (Tr) around 2000 was investigated in the Meteorological Research Institute (2008), where the source was estimated at ca. 370 m depth from the top of the 1909 lava dome, which lies at the center of the summit atrio. This unrest event was accompanied by a ground inflation (Tr1 in Table 2), both of which were probably caused by a common source (Meteorological Research Institute, 2008; Hashimoto *et al*., 2018).

Similar to Tokachidake's case, a prolonged demagnetization was also observed at the Ōana crater of Mt. Azuma, where phreatic eruptions have repeatedly occurred in historic times. Yamazaki *et al*. (2010), based on their repeated surveys from 2003 to 2009, obtained a demagnetizing source (Az) at ca. 300 m below the Ōana crater. This volcano also exhibited episodic ground inflations that were localized to the crater in a cycle of a few years (Yamazaki *et al*., 2010; Yoshida *et al*., 2012); these inflations are common in Tokachidake and Kuchinoerabujima.

Mt. Kusatsu-shirane is one of the most precisely monitored volcanoes having a long archive of geomagnetic total field records collected by the JMA since 1976. Takahashi and Fujii (2014) calculated the sources for two demagnetization events and five re-magnetization phases. In this study, we only dealt with the demagnetization events Ks1: 1982–85 and Ks2: 1988–91, both of which were sourced at a depth of ca. 500 m right below the Mizugama crater. Matsunaga *et al*. (2015), based on the records at four continuous stations operated by Tokyo Institute of Technology, discussed the demagnetization event Ks3 in May 2014. They estimated the source of this unrest event at a depth of 1,000–1,300 m, which was the deepest among those collected in this study. In addition, a relatively small moment change (~10^7 Am^2) in a short duration (about three weeks) corresponded to the largest moment rate (~10^8 Am^2/year). Note that the reliability of the source estimation for this particular event was somewhat doubtful because the maximum field change observed was 1.1 nT, which was close to a detection limit, and the number of sites used for source modeling was four, which is the same as the number of unknown parameters.

At Mt. Aso, geomagnetic monitoring has been performed by Kyoto University and the JMA since the 1980s. The 1st crater of Nakadake, one of the youngest cones, showed an elevated activity, including some Strombolian eruptions from the late 1980s to early 1990s. The crater has hosted a hot crater lake, which is locally called "Yudamari," since mid-1990s to early 2010s, during which ejection of muddy jets associated with small-scale phreatic explosions and red-hot incandescence at the crater wall were sometimes witnessed when the water level was low. The volcanic activity has elevated again since 2013 and evolved into a magmatic eruption in November 2014.

Tanaka (1993) precisely documented the elevated volcanic activity of Nakadake during 1989–1990, based on his frequently repeated magnetic surveys. The event As1 was a syn-eruptive unrest from September to November in 1989. In this period, a pit at the bottom of the 1st crater exhibited a flaming of 20–30 m height with ash emission, then followed by a Strombolian eruption, and finally by explosive eruptions in November. In contrast, As2 was a demagnetization event in a water-pool stage from February to April 1990, where the volcanic activity led to a phreatic eruption in the April. Both events were characterized by a shallow (ca. 200 m deep) demagnetization beneath the 1st crater of Nakadake. Tanaka (1993) interpreted that an effective demagnetization in the host rock was achieved by a convective heat transport due to a lateral flow of hot ground water around the conduit. Note that these demagnetization phases ended in explosive eruptions and immediately transited into a re-magnetizating phase. It was suggested that vent opening by explosions resulted in effective discharge of heat that had been accumulated in the shallow hydrothermal system in the preceding several months. Regarding the series of demagnetizing events As3 to As8 from 2001 to 2014, sources with similar depths (170 to 350 m) were obtained in the present study based on the continuous monitoring data by Kyoto University (2014, 2015). Note that the demagnetization was gradually, and sometimes episodically, built up in this period without exhibiting a remarkable re-magnetization phase. By referring to Hashimoto *et al*. (2001), which documented the geomagnetic field changes associated with volcanic activities in the 1990s, the 1st crater of Nakadake transited into the stage of a long-term demagnetizing trend. No remarkable re-magnetization was observed after the slight magnetizing phase in 2002–2003. Such a persistent one-way demagnetizing trend resulted in a considerable gap in the magnetic field between the current state (as of 2019) and mid-1990s. An open question is whether we can attribute such a one-way field change lasting over many years only to thermal demagnetization. We consider that the chemical demagnetization associated with hydrothermal alteration due to the recycling of lake water in the shallow subsurface right beneath the crater (Terada *et al*., 2012) may partly contribute to the process. An additional information on the example from this volcano is that no ground deformation that obviously synchronized with the demagnetization events was reported except for event As8.

At Kuchinoerabujima, an island volcano in southwestern Japan, Kyoto University deployed five continuous magnetic stations around the Shindake crater in 2000 and detected four distinct demagnetization events by 2010. Kanda *et al*. (2010) interpreted these events as indicative of a preparation process of a forthcoming phreatic eruption. According to their modeling, event Kc1 in 2001 was sourced at ca. 600 to 700 m depth right beneath the Shindake crater, which was clearly deeper and more intense than the following three events (Kc2 to Kc4). A remarkable feature of this unrest sequence was the episodically accelerated demagnetization with a few-year interval being devoid of an obvious re-magnetizing phase in between. The synchronized ground inflations with magnetic field changes were observed.

As mentioned in the previous section, geomagnetic field monitoring for volcanoes has been an unpopular attempt in countries outside Japan. Accordingly, only a limited number of field examples were found. Among them, we collected two events that were reported from White Island, New Zealand. Hurst and Christoffel (1973), based on their surveys repeated four times during 1970 to 71, estimated a demagnetization source (Wi1) at a very shallow part beneath the central crater. Likewise, Hashimoto *et al*. (2006) reported a demagnetizing source at ca. 400 m deep, based on their ground surveys performed in 2005 and 2006.

4. Ground deformation

In this study, we collected data for 19 unrest deformation events suggesting inflation from six volcanoes, all of which were modeled based on the Mogi model. We excluded deflation cases because we did not regard them as suggestive of unrest. We briefly reviewed these specific inflation events as follows. Event names in the main text are identical to the ones in Figs. 3 and 4 and Table 2, unless noted otherwise. An attention should be paid to the horizontal axis ranges of Figs. 3 and 4, which are different from those of Figs. 1 and 2.

At Tokachidake, the JMA, the Geological Survey of Hokkaido (GSH), and Hokkaido University have cooperated to repeat the GNSS surveys since 2003. A noticeable ground inflation started in 2006 and continued in the vicinity of the crater area of the 1926 and 1962 eruptions for over 10 years (Regional Volcanic Observation and Warning Center, Sapporo Regional Headquarters, JMA, 2018). The inflation, common to Kuchinoerabujima, exhibited episodic accelerations with a few-year interval, being devoid of an obvious deflation phase. According to the JMA's analysis in the reference above, the inflation source was estimated at a shallow depth either around the Taisho crater or around the 62-II crater, depending on the period analyzed.

At Mt. Tarumae, the JMA started the GNSS survey in 1999 in the summit atrio and kept performing annual campaigns. A quasi-isotropic and slow ground deformation was found with a modeled source at a shallow part right beneath the 1909 lava dome (Meteorological Research Institute, 2008; Hashimoto *et al*., 2018). A distinct inflation phase (Tr1) was observed around the year 2000, corresponding to the demagnetization event described in the previous section (Tr in Table 1). Besides this event, Koshiromaru (2014) investigated the tilt and strain changes that were precedential to the micro-earthquake swarm in July 2013. He estimated a relatively deep (ca. 4 km) inflation source (Tr2) 1.5 km north of the summit lava dome. The inflation source was adjacent to a micro-earthquake cluster and was suspected to be a part of the conduit.

At Mt. Azuma, Yoshida *et al*. (2012) investigated the GNSS records obtained by the JMA around the Ōana crater during 2002 to 2009. They reported three inflation events (Az1 to Az3) and two deflation events. The inflation and deflation repeated every few years at a depth of 300 to 1,000 m beneath the crater. Besides these unrest events, a relatively deep-sourced inflation was found based on the GNSS records from 2014 to 2015 (Az4: Tohoku University, 2015).

At Mt. Kusatsu-Shirane, an inflation centered at the Yugama crater was detected from March 2014 to November 2015 (Ks). The Mogi source, which was modeled by Tokyo Institute of Technology (2017) based on the tilt records had a moderate depth (540 to 840 m) as well as a moderate intensity (volume change) among the collected events. The volume rate of the event Ks in Table 2 and Fig. 4 was calculated by a simple division of the reported volume by the duration time. Taking the exponential decay in the tilt waveform of this particular event into account and using the earlier phase only, the volume rate is approximately doubled.

A series of events As1 to As3 at Mt. Aso referred to the estimation from particular GNSS baseline changes during the active period from 2014 to 2016 by Kyoto University (Ohkura *et al*., 2009), where the source location was assumed to be the same as the deflation source, which was modeled based on the precise leveling in the previous years. Among them, As1 corresponded to the period from July 2014 up to the initiation of a magmatic eruption on November 20, 2014. This inflation event was partly overlapped with the demagnetization event As1 shown in Figs. 1 and 2. The deformation events As2 and As3 preceded a phreatomagmatic eruption in September 2015 (Miyabuchi *et al*., 2018) and an explosion in October 2016, respectively. Although these two events had similarity to As1 in terms of the depth and volume, no demagnetization event was accompanied.

At Kuchinoerabujima volcano, seismic activity elevated from 1999 onward, and since then, the swarm of micro-seismicity and ground inflation localized to the Shindake crater began repeating with a few-year interval (Saito *et al*., 2015). In addition, some episodic demagnetization events were detected (Kanda *et al*., 2010) as shown in the previous section. Iguchi *et al*. (2007) obtained the spherical source models based on their GNSS repeated surveys. Event Kc1, sourced at ca. 600 m beneath the summit crater, was based on the changes between the campaigns in 1995/96 and 2000, and therefore, the timing and duration of the unrest were unknown. Events Kc2 and Kc3, the episodic inflations in 2005-06 and 2006-07, respectively, migrated upward with time. Remarkable inflations were also observed from September 2008 to February 2009. Saito *et al*. (2015) modeled these unrests based on the continuous records of GNSS and obtained double Mogi sources at different depths (Kc5a and Kc5b). In the present study, we cited the volume rate in the reference but did not convert it into volume for this particular event. In addition, Saito *et al*. (2015) mentioned that their double-source modeling was performed in order to evaluate how a deeper source could affect the displacement near the summit crater, and therefore, an accurate location or an inflation volume of each source was not significant. Besides, we added the spherical source of a finite volume (Kc4), that was modeled for the displacement between January 2006 and April 2014 based on the FEM calculation by Hotta and Iguchi (2017) for comparison. Event Kc4 was modeled to locate shallower than any other events of this volcano. Event Kc6 was based on the precise leveling that was conducted after the August 2014 eruption. The inflation event was attributed to a deep magmatic injection at 7,500 m depth prior to the eruption in May 2015 (Yamamoto *et al*., 2017).

A localized deformation was detected at the Numanotaira crater of Mt. Adatara from 1998 to 1999 by the GNSS repeated survey of the JMA. Yamamoto *et al*. (2008) obtained an inflating Mogi source at a very shallow depth (60 m) at the southwest crater wall (Ad in Figs. 3 and 4). However, model reliability of this event was unlikely to be high because modeling was performed with the records from only three sites except for the station of an assumed fixed point. According to their report, this unrest was followed by a subsequent deflation phase from 2001 to 2005 at the central part of the crater. Interestingly, the inflation–deflation sequence well-coincided with the sequence of thermal demagnetization followed by the cooling re-magnetization in the same period (Ad in Figs. 1 and 2).

5. Discussion

5-1 Characteristics of demagnetization and inflation sources

As is obvious from Figs. 1 to 4, a remarkable positive correlation is recognized between the source depth and source intensity (or its rate) both for the magnetism and the ground deformation. We examine this feature from the following three viewpoints.

First, we consider the problem related to the spatial scale of the monitoring network and point-source modeling. We suspect that the source depth intrinsically tends to be similar to the characteristic dimension of the monitoring network, so that the corresponding source intensity that meets the observed field changes is chosen. If so, the correlation in Figs. 1 to 4 is simply an apparent consequence reflecting the dimension of each monitoring network. Then, a void zone in a depth range of 1,000 to 3,000 m in Figs. 3 and 4 might be due to a lack of the monitoring network that has an appropriate dimension to detect the sources within such a depth range. On the contrary, if any physical entity showing a tight correlation between its depth and intensity (or its rate) does exist, it suggests a certain requirement from, for instance, a subsurface structure common to volcanoes that host a hydrothermal system. Currently, we do not have any definitive answer to this question. To solve this problem, we need a multiscale observation network that enables simultaneous detection of multiple sources with different depths, rather than the sophistication of the modeling itself.

Second, we discuss the problem related to a detection limit in the field observation. Naturally, the deeper the source is, the smaller is the field variation on the ground surface, given that the source intensity is fixed. In other words, a deep source cannot produce detectable signals on the ground surface in excess of the detection limits, unless it is fairly intense. Accordingly, there must be a cutoff line corresponding to the detection limit in an intensity-versus-depth scatter plot. Now, we check whether the linear correlations in Figs. 1 and 3 are due to the cutoff. In Fig. 1, eq. (1) is plotted with a dashed line as the detection limit corresponding to the demagnetization sources that produce a maximum total field change of 1 nT (reduction-to-pole equivalent) on the ground surface. Similarly, eq. (2) is plotted as the detection limit in Fig. 3 to indicate the inflation sources that produce a maximum uplift of 0.01 m on the ground surface.

$$\Delta M = \frac{2\pi \Delta F_{max}}{\mu_0} D^3 \qquad (1)$$

$$\Delta V = \frac{2\pi(\lambda + \mu)}{\lambda + 2\mu} D^2 \Delta h_{max} , \qquad (2)$$

where D, ΔM, ΔV, μ_0, ΔF_{max}, and Δh_{max} are the source depth, magnetic moment change, volume change, magnetic permeability in vacuum, maximum change in the total magnetic field, and maximum height change produced on the ground surface, respectively. The Lame's constants are indicated by λ and μ. As expected from eqs. (1) and (2), the slope of the detection limit lines in the log-log scale is 3 for magnetism and 2 for deformation. The detection limit of 1 nT adopted here is a typical value considering that the daily variations of the geomagnetic field have an amplitude of a few tens of nT, and that such variations of the extra-terrestrial origin are reduced to a few tenths by taking a simple difference from a reference station. Regarding the deformation, the detection limit is considered to be 0.01 m as a slightly smaller value than the typical vertical accuracy of GNSS repeated surveys, which is the basis of most collected events in this study. Note that it is practically possible to detect even smaller variations through other monitoring techniques such as continuous GNSS, precise leveling, high-sensitivity borehole tiltmeters, and strain meters.

For magnetism (Fig. 1), all currently compiled demagnetization events are above the detection limit, by an order of magnitude or more for most cases. That is, the signal-to-noise ratios of the magnetic unrest events collected here are generally quite high. Thus, the linear correlation in Fig. 1 is not the cutoff line due to the detection limit itself. Taking a closer look at the magnetic scatter plot in a depth range lower than 500 m, many events are larger than the detection limit by one to two orders of magnitude and no distinct correlation is observed between the depth and intensity. This is also the case with the rate-versus-depth plot (Fig. 2).

Regarding the deformation plot (Fig. 3), the three events at Mt. Aso during 2014 to 2016 (As 1 to As3) as well as the event at Mt. Tarumae in 2013 (Tr2) are plotted slightly below the detection limit. Of course, it does not mean that they are undetectable events but are based on a method with a higher sensitivity. As for As1 to As3, they are derived from the continuous GNSS records. Event Tr2 is based on the records by tiltmeters and strain meters in boreholes or a vault. An upward shift of the detection limit line seems to tie the events Kc3, Tr1, Az3, and Az4. This suggests that the detection limit of a repeated GNSS survey is not actually 0.01 m but larger by a few factors. If this is the case, the lower limit of the compiled events may correspond to the cutoff line due to the detection limit. Meanwhile, certain events such as Tk1, Tk2, and Kc1 considerably exceed the lower limit, indicating they are significant in either case.

Third, we focus on the difference between the intensity plots (i.e., Figs. 1 and 3) and the rate plots (i.e., Figs. 2 and 4). Correlation to the source depth is relatively higher in the latter than in the former. Especially, it is more obvious in the deformation plots. Looking at each individual event in detail, some relatively weak events in the intensity plot are shifted upward in the rate plot, and vice versa. In general, demagnetization and/or inflation in an unrest event are thought to accompany some relaxing processes such as the heat discharge from a vent and/or a lateral escape of causative fluids in the subsurface. In addition, near an active crater at some volcanoes, a characteristic sequence of unrest, in which episodic inflation is followed by a stagnant period without any recovering deflation phase, is repeated in an inter-eruptive period, as typically seen at Kuchinoerabujima in 2000s. Such a one-sided inflation implies a nonelastic deformation, where a cumulative volumetric change cannot always be attributed to the amount of pressure build-up. Accordingly, we consider that it is worth producing and comparing the two types of plots in evaluating the unrest events.

5-2 Anomaly evaluation

As pointed out in the previous section, a clear positive correlation was recognized between the source depth and source intensity (or its rate). Besides the physical reasoning for the correlation, we further investigated the scatter plots to examine an application for evaluating the severity of each individual unrest event, from the following three viewpoints.

5-2-1 Source depth

Let us first examine whether the source depth can be a useful proxy to the presence/absence of a subsequent eruption and the leading time to the eruption, if it exists. Regarding magnetism (Table 1, Figs. 1 and 2), the following events are accompanied by a subsequent eruption: Mp1 (Meakandake, 700 to 1,180 m, erupted in the middle of the unrest), As1 (Aso, 220m, erupted in the middle of the unrest), As2 (195 m, erupted in the waning phase of the unrest), As8 (350 m, erupted at the beginning of the unrest), and Wi1 (White Island, 200 m, erupted in the middle of the unrest). As for the events at Kuchinoerabujima, Kc1 is 610–754 m deep with 12 years of preceding time, Kc2 is 95–273 m deep with 10 years, Kc3 is 78–262 m with 8 years, and Kc4 is 137–229 m with 7 years, given that all of them can be regarded as the unrest events leading to the 2014 eruption. As indicated by Kanda *et al*. (2010), Kc1 is clearly deeper than the other three unrests, so the demagnetization is likely to have migrated upwards at a certain stage in the preparation process to 2014 eruption. All above events accompanied by a subsequent eruption are circled in Figs. 1 and 2. Although most events are relatively shallow, except for Mp1 and Kc1, it seems difficult to conclude that shallow unrests always bring an eruption, because there are also a certain number of unerupted events with a shallow source depth.

Next, we move on to the deformation (Table2, Figs. 3 and 4). Following are the erupted unrests: As1 (Aso, 5,000 m, erupted in the early stage of the unrest), As3 (5,000 m, erupted in the early stage of the unrest), Kc1 (Kuchinoerabujima, 600 m, erupted after 14 to 19 years from the unrest), Kc2 (300 m, erupted after 8 to 9 years), Kc3 (130 m, erupted after 7 to 8 years), Kc4 (100 m, erupted after 0.5 to 8 years), Kc5a/5b (100 and 600 m, respectively after 5 to 6 years), and Kc6 (7,500 m, after 2 to 9 months). These events are circled in Figs. 3 and 4. Note that the inflation has migrated upward on the way to the 2014 eruption, as seen for demagnetization. However, the inflation source Kc6 detected by the precise leveling between the 2014 and 2015 eruptions is undoubtedly deeper than other sources. Yamamoto *et al*. (2017) interpreted that Kc6 was an inflation of magmatic origin. We consider that the physical entity of this particular event differs from other events prior to the phreatic eruption in 2014. If we exclude Kc6 as well as As1 to 3, which are also plausibly magmatic from the current consideration, the remaining non-magmatic unrests seem to form a relatively shallow group. However, these unrest events were tied to a single common eruption at Kuchinoerabujima in 2014. Moreover, there are shallow unrest events without a subsequent eruption, as well as deep-sourced erupted events. Considering these facts, we reach the same conclusion as that for magnetism: it is difficult to discriminate the unrest events that result in a subsequent eruption based solely on the source depth.

5-2-2 Deviation from the correlation trend

As the next investigation, we examine the scatter plots from the viewpoint of anomaly evaluation based on the deviation from the correlation trend. Looking again at the scatter plot for the demagnetizing moment rate (Fig. 2), "erupted" unrest events As1 and As2 (Aso 1989–90), Kc2 to Kc4 (Kuchinoerabujima 2003–2007), and Wi1 (White Island 1970) lie in a somewhat deviated region upper-leftward from the overall linear trend. Especially, As1 is distinctive, after which the magmatic activity in 1989 became intense. Meanwhile, As8, a demagnetization event prior to the magmatic eruption in 2014, lies on the overall trend and does not seem to be anomalous, although it has a relatively large moment rate among the series of unrest events from 2000 onward. Event Mp1, during which a phreatic eruption occurred in November 2008 at Mt. Meakandake, as well as Ks3 at Mt. Kusatsu-Shirane accompanying an inflation, are right on the trend, although they are outstandingly deep and strong. Noticeably, six out of nine shallow unrests that deviate upper-left from the linear trend are the erupted events. Furthermore, the erupted unrests As1, As2, and As8 shift upward in the rate plot (Fig. 2) as compared to the adjacent events in the moment plot (Fig. 1). In contrast, future progress of the "so-far unerupted" event Az at Mt. Azuma should be carefully watched because it is plotted in the lowermost position in the moment rate plot, even though it has a relatively large cumulative moment.

Let us now proceed to the deformation rate plot (Fig. 4), which clearly shows that deformation is more neatly correlated as compared to magnetism. None of the events seem obviously deviated from the trend line. Looking at the inflation volume plot (Fig. 3), the ongoing events Tk1 and Tk2 at Tokachidake are plotted in the upper part as compared to events Kc2 and Kc3 at Kuchinoerabujima, which have similar depths but are followed by an eruption in 2014. However, these event at Tokachidake markedly shift downward in the rate plot (Fig. 4). This is a consequence of the slow inflation with a long duration (over a decade) at Tokachidake. On the contrary, the two events at Mt. Azuma (Az1 and Az3) are plotted at a higher position in the rate plot than in the volume plot as compared to other events with similar source depths. We consider that future progress of the volcanic activities at these two volcanoes will be an important clue to improve the evaluation criteria of the unrest events.

5-2-3 Consideration from imaginary events

The number of unrest events collected in this study is still limited, and thus, we do not consider that we have yet clarified the whole picture. To proceed the discussion a little further, let us consider the imaginary events plotted in the region far outside the trend on the scatter plots. What do they mean, if they exist?

At first, we consider the lower-right domain in the scatter plots, where the relevant unrest events are deep and week (or sluggish). Such events, even if they occurred, are not observable as they are too weak to be detected from the ground surface, especially through campaign surveys of the total magnetic field or GNSS. For this reason, we call these events as "undetected unrests" in Fig. 5. As we know, deformation and oscillation, which are generally termed as the VLP signals in seismology with a smaller amplitude and a shorter duration (typically a timescale from 10 to 1,000 sec), are reported from many volcanoes through high-sensitivity tiltmeters, strain meters, and broadband seismometers. As is easily imagined, most of such tiny events may occupy the lower-right domain in the intensity-versus-depth scatter diagram, if plotted together. However, this is not necessarily the case, if they are converted into the rate plot because they have generally a very short duration. Currently, we do not know whether such VLP events have any physical relationship with the unrest events with a longer lifetime than what we are dealing with in this study. Does repetition of VLP events trigger a larger and longer event? Is a larger unrest an accumulation of the tiny changes due to an individual VLP event? These are one of the issues to be investigated in the future.

On the other hand, it is intuitively natural to consider that very strong unrest events close to the ground surface are likely to cause an eruption. Such unrest events should be plotted in the upper-left triangular domain in Fig. 5, if they do exist. This domain is blank in the scatter plot of the actual events collected in this study (Fig. 4), implying that such very shallow and strong unrest events are, in principle, detectable, but are physically impossible or have never been observed for some reasons; for example, they occur very rarely. Alternatively, they might have erupted before we observed such strong shallow events whose source body emerges partly out the ground surface, where a point source modeling itself is probably inappropriate, as well.

As a consequence, we assert that the observable unrest events should be plotted within a diagonal band between the lower-right and upper-left domains in a scatter plot, as illustrated in Fig. 5. We can divide the unrest events in this intermediate zone into two groups: "unerupted" and "erupted." Based on the discussion above, more deviated unrest events towards the upper-left in the scatter plot have a higher probability of a subsequent eruption. Conceptually, it indicates that a source becomes even stronger, or migrates upward to form an even shallower source, when the causative fluid is supplied in excess to the possible relaxation due to lateral flows in a shallow hydrothermal system. In such cases, the relevant source should migrate upward or leftward in Figs. 1 or 3. Another possible situation is the hydrothermal sealing or conduit obstruction, in which the permeability in the conduit is depleted due to deposition of hydrothermal alteration mineral assemblage in rock pores (Christenson *et al*., 2010). Such a process has an effect of reducing the lateral and/or upward transport of the fluids, resulting in an intensified source at the same location (e.g. Tanaka *et al*., 2017, 2018). In this case, such a source should shift upward in the scatter plot with time.

It is somewhat inevitable that some variability due to specific characteristics of an individual volcano is mixed in the scatter plots based on the events from multiple volcanoes. Regarding the magnetism, for example, the initial rock magnetization can range in one or two orders. Accordingly, "erupted unrests" and "unerupted unrests" may be mixed in the "intermediate zone" in Fig. 5. Nonetheless, we expect that some statistical or probabilistic imminence evaluation for a forthcoming eruption will be realized in the future when sufficient number of events have been accumulated and sufficiently dense event distribution, as schematically illustrated in Fig. 5, has been obtained.

Although not included in the present compilation, some localized and very shallow ground inflations have been observed to be associated with the recent phreatic eruptions at Mt. Hakone in 2015 (Kobayashi *et al*., 2018) and at Iwo-yama, Kirishima Volcanic Group in 2018 (Tsukamoto *et al*., 2018). In the latter example, the geometry of a low-resistivity clay layer at a shallow part below the eruption site was imaged by the magnetotellurics, and then compared with the two deformation sources at the top and bottom of the clay layer. They interpreted the clay layer as an impermeable seal that covered an underlying hydrothermal reservoir, corresponding to the deeper inflation source. They considered that a partial failure of the seal zone resulted in another inflation source at a very shallow depth. This is an important clue to improve the severity evaluation of non-magmatic unrest events to compare such a well-studied example to other unrest sources at other volcanoes in terms of depth and deformation rate in a time sequence leading up to the eruption.

6. Conclusions

In the present study, we collected non-magmatic unrest events mainly from Japanese volcanoes that have been monitored for an extended time period. Based on a bibliographic survey with some individual modeling by ourselves, we compiled the demagnetization and inflation events whose sources were obtained from a single dipole model and the Mogi model for magnetism and deformation, respectively. Then, we produced the scatter plots between the source intensity or its rate with respect to the source depth. Remarkable positive correlations were found in both magnetism and deformation. We clarified that most magnetic events and some deformation events were clearly plotted above the cutoff lines related to the envisaged detection limits. Meanwhile, we suspected that the characteristic dimension of the monitoring networks and/or uncertainty in the simplified point-source modeling may have contributed to producing an apparent correlation between the source depth and intensity.

On the source intensity- (or its rate-) versus-depth scatter plot, there may have been numerous “undetected unrest” sources in the lower-right domain, which was actually left blank. However, we considered that the upper-left domain was probably the region of physically impossible sources or those with an extremely low occurrence probability. As far as the events collected in the present study are concerned, no remarkable relationship was found between the source depth and the presence/absence of a subsequent eruption. We proposed the concept of statistical severity evaluation of an individual unrest event by measuring the upper-leftward deviation from the linear trend on the scatter plots, although the number of events was not sufficient at this moment. Further event accumulation through literature surveys, as well as field observations in the future, is necessary to verify this hypothesis. In addition, any other source parameters that characterize the non-magmatic unrest may facilitate the statistical evaluation of the anomaly, as they increase the dimension of data space used for the evaluation.

In the present study, we only collected the reported events based on point-source modeling, where we did not take physical properties into account. Of course, the model that could explain the field data was not unique. Therefore, care must be taken in interpreting the sources collected here, as they may not accurately represent the physical entities, even if they qualitatively reflect time variations of a hydrothermal system at individual volcanoes. To develop a statistical approach that we proposed here into an evaluation technique of eruption imminence in the future, collaboration with numerical modeling that facilitates us to interpret the field data on the ground in relation to the subsurface processes in a hydrothermal system will be important, where subsurface inhomogeneity and temporal evolution of the system are incorporated.

Acknowledgments

We are grateful to H. Aoyama and R. Tanaka of Hokkaido University and M. Ichiki of Tohoku University for their valuable discussion. This study was partly supported by the

Ministry of Education, Culture, Sports, Science and Technology (MEXT) of Japan, under its Earthquake and Volcano Hazards Observation and Research Program. Constructive comments from K. Aizawa and an anonymous reviewer greatly contributed to improving the manuscript.

References

Barberi, F., Bertagnini, A., Landi, P. and Principe, C. (1992) A review on phreatic eruptions and their precursors. *J. Volcanol. Geotherm. Res.*, **52**, 231-246, doi:10.1016/0377-0273(92)90046-G.

Browne, P. R. L. and Lawless, J. V. (2001) Characteristics of hydrothermal eruptions, with examples from New Zealand and elsewhere. Earth-Science Rev. **52**, 299-331.

Christenson, B., Reyes, A. G., Young, R., Moebis, A., Sherburn, S., Cole-Baker, J. and Britten, K. (2010) Cyclic processes and factors leading to phreatic eruption events: Insights from the 25 September 2007 eruption through Ruapehu Crater Lake, New Zealand. *J. Volcanol. Geotherm. Res*., **191**, 15-32, doi: 10.1016/j.jvolgeores.2010.01.008.

De Moor, J. M., Aiuppa, A., Pacheco, J., Avard, G., Kern, C., Liuzzo, M., Martínez, M., Giudice, G. and Fischer, T. P. (2016) Short-period volcanic gas precursors to phreatic eruptions: Insights from Poás Volcano, Costa Rica. *Earth Planet. Sci. Lett.*, **442**, 218-227, doi: 10.1016/j.epsl.2016.02.056.

Hashimoto, T., Aoyama, H., Koyama, H., Morii, A., Mishima, W., Ogino, T., Takahashi, R., and Okazaki, N. (2018) Importance of multi-disciplinary monitoring during inter-eruptive periods -A case study from Mt. Tarumae-, Monthly Chikyu, **40**, 163-169 (in Japanese).

Hashimoto, T., Kanda, W., Hurst, A. W., Utsugi, M., and Yoshimura R. (2006) Repeated magnetic surveys on White Island. Report of Grant-in-aid for Scientific Research B2 No.1543007 (2003-2005), 1-43 (in Japanese).

Hashimoto, T., Nishimura, M., Arita, S., Yamamoto, T., Ogiso, M., Shigeno, N., Okazaki, N. and Mogi, T. (2010) Heat accumulation beneath Tokachidake volcano as inferred from magnetic changes. *Geophys. Bull. Hokkaido Univ*., **73**, 269-280, doi:10.14943/gbhu.73.269.

Hashimoto, T., Tanaka, Y. and Utsugi, M. (2001) Geomagnetic variation observed at Aso Volcano during the past ten years. *Annual. Disast. Res. Inst., Kyoto Univ.*, **44** (B-1), 333-343, http://hdl.handle.net/2433/80511 (in Japanese with English abstract).

Hotta, K. and Iguchi, M. (2017) Ground deformation source model at Kuchinoerabu-jima volcano during 2006–2014 as revealed by campaign GPS observation. *Earth Planets Space*, **69**: 173, doi:10.1186/s40623-017-0763-7.

Hurst, A. W. and Christoffel, D. A. (1973) Surveillance of White Island Volcano, 1968–1972. *New Zealand J. Geol. Geophys.*, **16**, 965-972, doi:10.1080/00288306.1973.10555236.

Iguchi, M., E. Saito and Suzuki, A. (2007) Repeated GPS Measurements at Kuchinoerabujima volcano during the Period from 1995 to 2006. In *Practical Study on Prediction of Phreatic Eruption and Its Change at Kuchinoerabujima Volcan, Japan, Disast. Prev. Res. Inst., Kyoto Univ.*, 33-40, http://www.svo.dpri.kyoto-u.ac.jp/H18kuc/05_iguchi.pdf (in Japanese).

Kanda, W., Utsugi M., Tanaka, Y., Hashimoto, T., Fujii, I., Hasenaka, T. and Shigeno, N. (2010) A heating process of Kuchi-erabu-jima volcano, Japan, as inferred from geomagnetic field variations and electrical structure. *J. Volcanol. Geotherm. Res.*, **189**, 158-171, doi:10.1016/j.jvolgeores.2009.11.002.

Seismology and Volcanology Research Department, Meteorological Research Institute (2008) Studies on Evaluation Method of Volcanic Activity. *Tech. Rep. Meteorol. Res. Inst.*, **53**, 286-303, doi:10.11483/mritechrepo.53. (in Japanese with English abstract).

Koshiromaru, T. (2014) Pressure Source Model Inferred from Tilt and Strain Changes Preceding the Seismic Swarm Beneath Tarumae Volcano During June and July 2013. Master Thesis, Grad. Sch. Sci., Hokkaido Univ., pp. 89 (in Japanese).

Graduate School of Science, Kyoto University (2014) Geomagnetic Total Field Observation at Aso Volcano (~ Sep. 2014). In *The 130th Coordinating Committee for Prediction of Volcanic Eruption* (9) *Kyushu district and Nansei islands*, 29 (in Japanese).

Graduate School of Science, Kyoto University (2015) Geomagnetic Total Field Observation at Aso Volcano (~ Dec. 2014). In *The 131st Coordinating Committee for Prediction of Volcanic Eruption* (4) *Mt. Aso*, 29 (in Japanese).

Kobayashi, T., Morishita, Y. and Munekane, H. (2018) First detection of precursory ground inflation of a small phreatic eruption by InSAR, *Earth Planet. Sci. Lett.*, **491**, 244-254, doi: 10.1016/j.epsl.2018.03.041.

Mastin, I. (1991) The roles of magma and groundwater in the phreatic eruptions at Inyo Craters, Long Valley Caldera, California. *Bull. Volcanol.*, **53**, 579-596.

Matsunaga, Y., Kanda, W., Koyama, T. and Ogawa, Y. (2015) Geomagnetic Changes During the 2014 Activity of Kusatsu-Shirane Volcano, *Proceedings of Conductivity Anomaly Research Symposium 2015*, 67-74 (in Japanese).

Miyabuchi, Y., Iizuka, Y., Hara, C., Yokoo, A. and Ohkura, T. (2018) The September 14, 2015 phreatomagmatic eruption of Nakadake first crater, Aso Volcano, Japan: Eruption sequence inferred from ballistic, pyroclastic density current and fallout deposits. *J. Volcanol. Geotherm. Res.*, **351**, 41-56, doi: 10.1016/j.jvolgeores.2017.12.009.

Ohkura, T. *et al*. (2009) Precise Leveling Survey in Aso Caldera (Sep. - Oct. 2008). In *Report of the 4th Integrated Comprehensive Observation of Aso Volcano*, 8-15 (in Japanese), http://www.aso.vgs.kyoto-u.ac.jp/shuchu/02.pdf.

Rouwet, D. and Morrissey, M. M. (2015) Mechanisms of crater lake breaching eruptions. In *Volcanic Lakes* (Rouwet, D., Christenson, B., Tassi, F. and Vandemeulebrouck, J. eds), 73-91, Springer-Heidelberg.

Rouwet, D., Sandri, L., Marzocchi, W., Gottsmann, J., Selva, J., Tonini, R. and Papale, P. (2014) Recognizing and tracking volcanic hazards related to non-magmatic unrest: a review. *J. Appl. Volcanol.*, **3**:17, doi:10.1186/s13617-014-0017-3.

Saito, E., Iguchi, M. and Matsushima, N. (2015) Ground deformation revealed by GPS observation for 10 years before the 2014 eruption in Kuchinoerabujima volcano. *Bull. Geol. Surv. Japan*, **66**, 5/6, 103–141, doi:10.9795/bullgsj.66.103.

Regional Volcanic Observation and Warning Center, Sapporo Regional Headquarters, JMA (2018) Volcanic Activity of Tokachidake Volcano During the Last 10 Years (2006-2016). *Report of Coordinating Committee for Prediction of Volcanic Eruption*, **127**, 29-44 (in Japanese). https://www.data.jma.go.jp/svd/vois/data/tokyo/STOCK/kaisetsu/CCPVE/Report/127/kaiho_127_05.pdf

Stix, J. and de Moor, J. M. (2018) Understanding and forecasting phreatic eruptions driven by magmatic degassing. *Earth Planets Space*, **70**:83, doi:10.1186/s40623-018-0855-z.

Takahashi, K. and Fujii, I. (2014) Long-term thermal activity revealed by magnetic measurements at Kusatsu-Shirane volcano, Japan. *J. Volcanol. Geotherm. Res.*, **285**, 180-194, doi: 10.1016/j.jvolgeores.2014.08.014.

Takahashi, K., Takakura, S., Matsushima, N. and Fujii, I. (2018) Relationship between volcanic activity and shallow hydrothermal system at Meakandake volcano, Japan, inferred from geomagnetic and audio-frequency magnetotelluric measurements. *J. Volcanol. Geotherm. Res.*, **349**, 351-369.

Tanaka, Y. (1993) Eruption mechanism as inferred from geomagnetic changes with special attention to the 1989-1990 activity of Aso Volcano. *J. Volcanol. Geotherm. Res*., **56**, 319-338.

Tanaka R., Hashimoto, T. and Suzuki, A. (2016) Magnetic total field changes and thermal activity around Nakamachineshiri crater, Meakandake. *Geophys. Bull. Hokkaido Univ.*, **79**, 15-23 (in Japanese with English abstract), doi:10.14943/gbhu.79.15.

Tanaka, R., Hashimoto, T. Matsushima, N. and Ishido, T. (2017) Permeability-control on volcanic hydrothermal system: case study for Mt. Tokachidake, Japan, based on numerical simulation and field observation. *Earth, Planets, Space*, **69**:39, doi: 10.1186/s40623-017-0623-5.

Tanaka, R., Hashimoto, T., Matsushima, N. and Ishido T. (2018) Contention between supply of hydrothermal fluid and conduit obstruction: inferences from numerical simulations. *Earth, Planets, Space*, **70**:72, doi: 10.1186/s40623-018-0840-6.

Terada, A., Hashimoto, T. and Kagiyama, T. (2012) A water flow model of the active crater lake at Aso volcano, Japan: fluctuations of magmatic gas and groundwater fluxes from the underlying hydrothermal system. *Bull. Volcanol*., **74**, 641-655, doi: 10.1007/s00445-011-0550-4.

Tsukamoto, K., Aizawa, K., Chiba, K., Kanda, K., Uyeshima, M., Koyama, T., Utsugi, M., Seki, K. and Kishita, T. (2018) Three-dimensional resistivity structure of Iwo-yama volcano, Kirishima volcanic complex, Japan: relationship to shallow seismicity, surface uplift, and a small phreatic eruption. *Geophys. Res. Lett*., **45**, 12821-12828, doi:10.1029/2018GL080202, 2018.

Tohoku University (2015) Ground Deformation around Mt. Azuma. In *The 131st Coordinating Committee for Prediction of Volcanic Eruption* (8) *Tohoku District*, 104-106 (in Japanese).

Tokyo Institute of Technology (2017) Ground Deformation and Thermal Activities at Mt. Kusatsu-Shirane, In *The 138th Coordinating Committee for Prediction of Volcanic Eruption* (6) *Kusatsu-Shirane and Aso*, 22-23 (in Japanese).

Yamamoto, K., Ohkura, T., Yokoo, A., Tameguri, T., Sonoda, T. and Inoue, H. (2017) Vertical ground deformation related to the 2014 and 2015 eruptions at Kuchierabujima Volcano, Japan detected by repeated precise leveling surveys. *J. Nat. Disast. Sci*., **38**, 133-144.

Yamamoto, T., Takagi, A. Fukui, K. and Owada, T. (2008) Hydrothermal Activity Inferred from Comprehensive Observation of Unrest in Adatara Volcano. *Pap. Meteorol. Geophys*., **59**, 39-64 (in Japanese with English abstract), doi:10.2467/mripapers.59.39.

Yamazaki, A. *et al*. (2010) Electromagnetic Observations at the Azuma Volcano, Proceedings of *Conductivity Anomaly Research Symposium 2010*, 5-11 (in Japanese with English abstract). http://www.eqh.dpri.kyoto-u.ac.jp/CA/2010/Yamazaki_et_al_CA2010.pdf.

Yoshida, Y., Funakoshi, M., Nishida, M., Ohmi, K., Takagi, A. and Ando, S. (2012) Crustal Deformation Observed by GPS around Azuma Volcano. *Quarterly J. Seismol.*, **76**, 1-8 (in Japanese with English abstract), https://www.jma.go.jp/jma/kishou/books/kenshin/vol76p001.pdf.

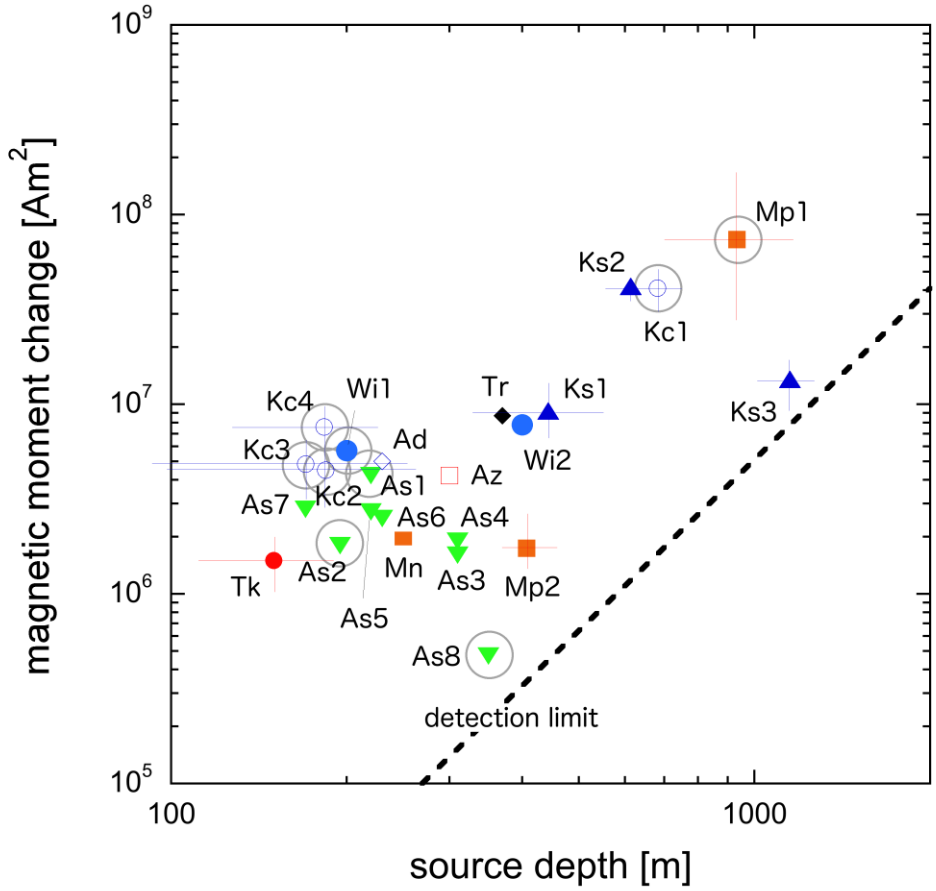

Fig. 1 Magnetic moment changes assuming a single dipole model, based on the reported geomagnetic total field records. Event names and references are listed in Table 1. The horizontal axis indicates the source depth from the ground surface. The dashed line represents a virtual detection limit calculated from the demagnetization sources that produce a maximum total field change of 1 nT on the ground surface. “Erupted” events are circled in gray.

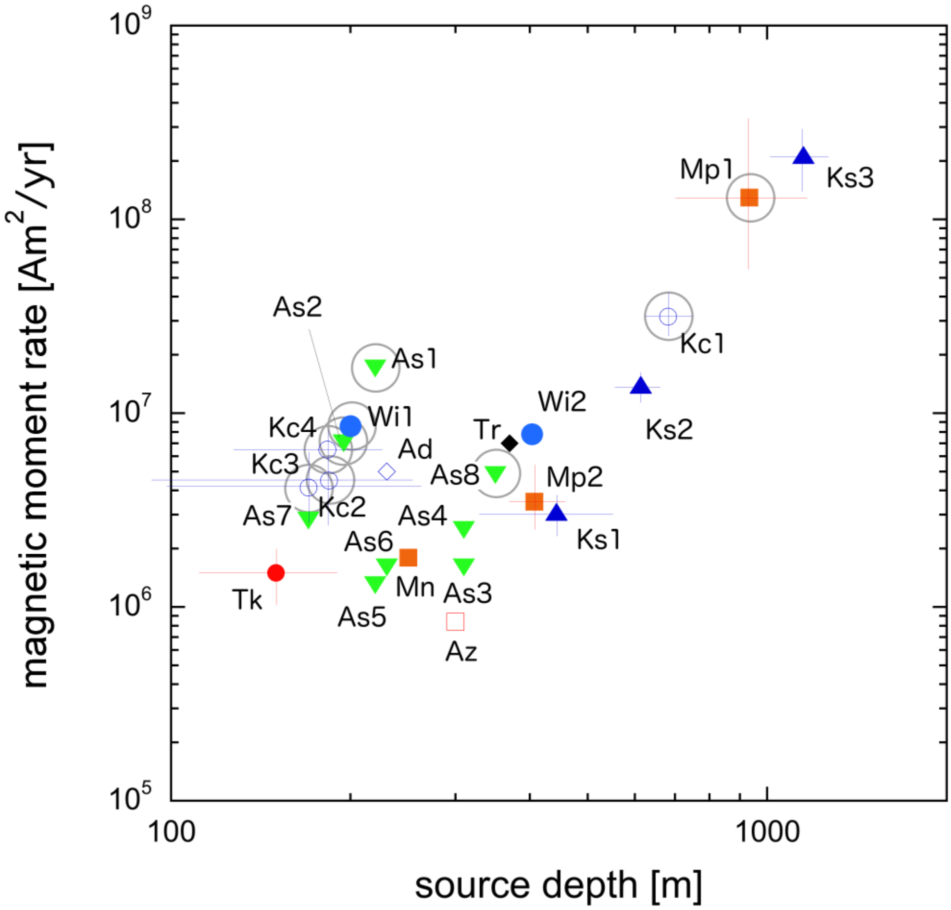

Fig. 2 Magnetic moment rates assuming the single dipole model, based on the reported geomagnetic total field records. The moment rate is plotted in units of Am^2/yr. The horizontal axis indicates the source depth from the ground surface. Event names and references are listed in Table 1. "Erupted" events are circled in gray.

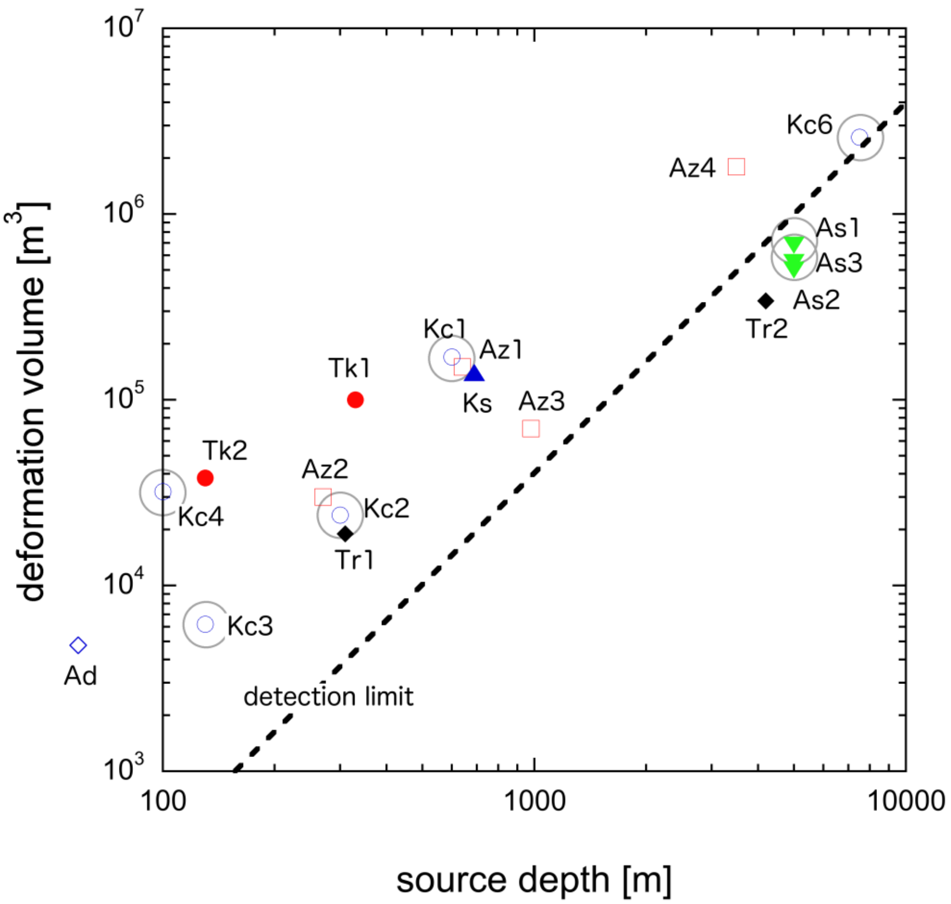

Fig. 3 Source volume changes estimated from the Mogi model, based on the reported deformation records. The horizontal axis indicates the source depth from the ground surface. Event names and references are listed in Table 2. Kc4 is based on FEM modeling by Hotta and Iguchi (2017). The dashed line represents a virtual detection limit calculated from the inflation sources that produce a maximum uplift of 1 cm on the ground surface. “Erupted” events are circled in gray.

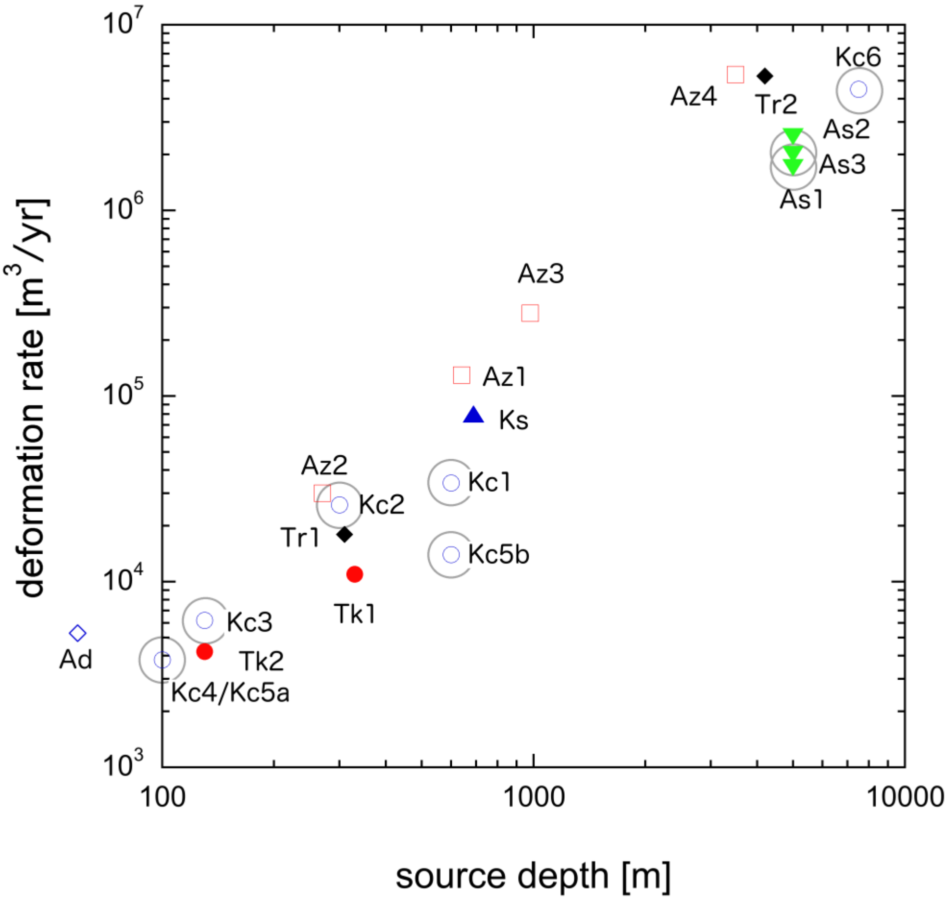

Fig. 4 Source volume rates estimated from the Mogi model, based on the reported deformation records. The volume rate is plotted in units of m^3/yr. The horizontal axis indicates the source depth from the ground surface. Event names and references are listed in Table 2. “Erupted” events are circled in gray.

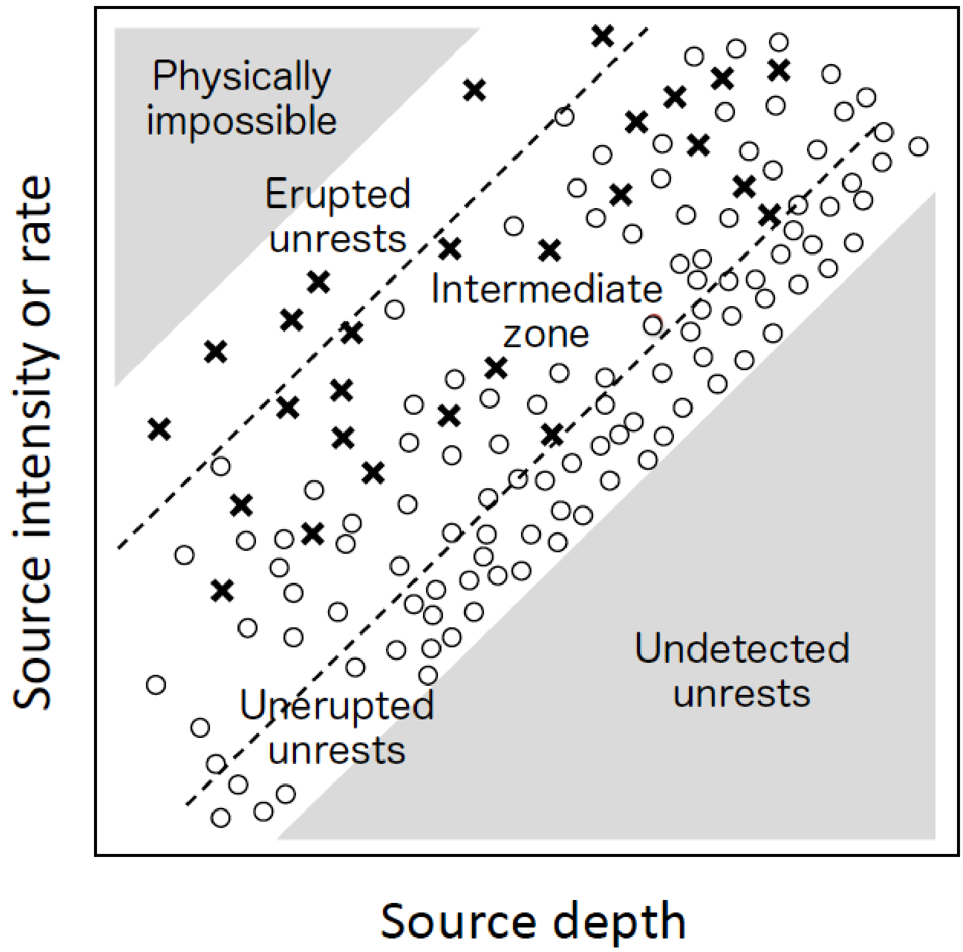

Fig. 5 Conceptual scatter plot demonstrating the statistical evaluation of non-magmatic unrest events. The symbols × and ○ represent "erupted" and "unerupted" unrests, respectively. Both kinds occur in the intermediate zone between the two dashed lines. Very small events at great depths, which belong in the shaded triangular zone on the lower-right, are not observable (undetected unrests). Very strong events close to the ground surface, which belong in the shaded triangle on the upper-left, are physically impossible.

Table 1 References for the demagnetization events and their source parameters plotted in Figs. 1 and 2. The second right column indicates the interpretation of the demagnetization source in the literature (P: hydrothermal system, M: magma, U: undefined).

Volcano name Crater name	event name	period of analysis	references	source depth (m)	magnetic moment change (Am^2)	magnetic moment rate (Am^2/yr)	origin	remarks
Meakandake Pon-machineshiri cr.	Mp1	2008.09-2009.09 (*1)	Takahashi *et al.* (2018)	700-1180 (*2)	2.7×10^{7}- 1.8×10^{8}	5.4×10^{7}-3.6×10^{8} (*3)	P	(*1) Phreatic eruption on Nov. 18, 2008 (*2) Converted by us into the depth from the 96-1 crater (1375m) (*3) Calculated by us using the early phase in the continuous record (2008.11-2009.04 and 2013.07-12)
	Mp2	2013.06-2014.06		370-470 (*2)	$1.3\text{-}2.7\times10^{6}$	$2.6\text{-}5.4\times10^{6}$ (*3)	P	
Meakandake Naka-machineshiri cr.	Mn	2014.08-2015.09	Tanaka *et al.* (2016)	250	2×10^{6}	1.8×10^{6}	P	Modeling based on the differential field in two repeat surveys
Tokachidake 62-2 cr.	Tk	2008.09-2009.09	Hashimoto *et al.* (2010)	110-190 (*4)	$1.0\text{-}2.0\times10^{6}$	$1.0\text{-}2.0\times10^{6}$	P	Modeling based on the field trends in three repeat surveys (*4) Depth measured from the bottom of the 62-2 crater (1730m)
Tarumae summit cr.	Tr	1999.07-2000.10	Meteorol. Res. Inst. (2008)	370 (*5)	8.7×10^{6}	7.0×10^{6} (*6)	P	(*5) Converted by us into the depth from the top of the 1909 lava dome (1041m) (*6) Calculated by us based on the differential field in two surveys
Azuma Oana cr.	Az	2004-2009	Yamazaki *et al.* (2010)	300	4.2×10^{6}(*7)	8.4×10^{5} (*7)	P	(*7) Converted by us from the moment change, based on the volume and the assumed magnetization shown in the reference
Adatara Numano-Taira cr.	Ad	1997.07-1998.06	Yamamoto *et al.* (2008)	230	5×10^{6}	5×10^{6} (*8)	P	(*8) Converted by us from the moment change divided by the analysis period
Kusatsu-Shirane around Mizugama cr.	Ks1	1982.11-1985.10	Takahashi and Fujii (2014)	326-560 (*9)	6.6×10^{6}- 1.2×10^{7}	$2.2\text{-}3.9\times10^{6}$ (*10)	P	(*9) Converted into the depth from the bottom of Mizugama crater (2056m) (*10) Converted by us from the moment change divided by the analysis period
	Ks2	1988.09-1991.09		551-677 (*9)	$3.6\text{-}4.8\times10^{7}$	$1.2\text{-}1.6\times10^{7}$ (*10)	P	
	Ks3	2014.05.08-2014.05.31	Matsunaga *et al.* (2015)	1000-1300	$0.9\text{-}1.8\times10^{7}$	$1.4\text{-}2.9\times10^{8}$ (*11)	P	Modeling based on the four continuous stations (*11) Converted by us from the moment change divided by the analysis period

Aso Nakadake 1st cr.	As1	1989.09- 1989.11 (*12)	Tanaka (1993)	220 *(13)	4.2×10^6 (*14)	1.7×10^7 (*15)	M	Modeling based on weekly to monthly repeated surveys at 15 sites (*12) Strombolian eruption stage (*13) Converted by us into the depth from the SW rim of the 1st crater (1270m) (*14) Converted by us from the moment change, based on the volume and the assumed magnetization in the reference (*15) Converted by us from the moment change divided by the analysis period (*16) Water pool stage (phreatic eruption at the end of the period)
	As2	1990.02- 1990.04 (*16)		195 *(13)	1.8×10^6 (*14)	7.0×10^6 (*15)	P	
	As3	2001.01- 2001.12	Fac. Sci., Kyoto Univ. (2014)	310 (*17)	1.6×10^6	1.6×10^6	P	Sources were obtained in this study by using the records at four continuous stations operated by Kyoto university (*17) Depths measured from the southwestern rim of the 1st crater (1270m)
	As4	2003.01- 2003.09		310 (*17)	1.9×10^6	2.5×10^6	P	
	As5	2007.01- 2008.12		220 (*17)	2.7×10^6	1.3×10^6	P	
	As6	2009.10- 2011.04		230 (*17)	2.5×10^6	1.6×10^6	P	
	As7	2013.01- 2013.12	Fac. Sci., Kyoto Univ. (2015)	170 (*17)	2.8×10^6	2.8×10^6	P	
	As8	2014.10.02- 2014.11.25		350 (*17)	4.7×10^5	4.8×10^6	M	
Kuchinoerabujima Shindake cr.	Kc1	2001.05- 2002.07	Kanda *et al.* (2010)	610-754 (*18)	$3.0\text{-}5.2\times10^7$ (*19)	$2.4\text{-}4.1\times10^7$ (*20)	P	(*18) Converted by us into the depth from Shindake crater (495m) (*19) Estimations based on the records at five continuous stations (*20) Converted by us from the moment change divided by the analysis period
	Kc2	2003.06- 2004.06		95-273 (*18)	$2.9\text{-}6.8\times10^6$ (*19)	$2.7\text{-}6.3\times10^6$ (*20)	P	
	Kc3	2004.12- 2006.01		78-262 (*18)	$3.1\text{-}6.6\times10^6$ (*19)	$2.6\text{-}5.7\times10^6$ (*20)	P	
	Kc4	2006.09- 2007.10		137-229 (*18)	$5.3\text{-}9.9\times10^6$ (*19)	$4.5\text{-}8.5\times10^6$ (*20)	P	

White Island (NZ) 1933 cr.	Wi1	1970.11-1971.07	Hurst and Christoffel (1973)	200	5.7×10^6 (*21)	8.6×10^6 (*21)	P	Modeling based on four repeat surveys (*21) Calculated by us based on the demagnetized volume, assumed magnetization, and the analysis period in the reference
	Wi2	2005.02-2006.02	Hashimoto *et al*. (2006)	400	7.8×10^6	7.8×10^6	P	Modeling based on two repeat surveys

Table 2 References for the ground inflation events and their source parameters plotted in Figs. 3 and 4. The second right column indicates the interpretation of the inflation source in the literature (P: hydrothermal system, M: magma, U: undefined).

Volcano name Crater name	event name	period of analysis	references	source depth (m)	source volume change (m^3)	source volume rate (m^3/yr)	origin	remarks
Tokachidake Taisho cr.	Tk1	2005.06- 2014.06	Sapporo District Meteorological Observatory (2018)	330 (*1)	1.0×10^5 (*2)	1.1×10^4	P	(*1) Depth measured from the bottom of the 62-2 crater (1730m) (*2) Converted by us from the moment rate multiplied by the analysis period
Tokachidake 62-2 cr.	Tk2	2005.06- 2014.06		130 (*1)	3.8×10^4 (*2)	4.2×10^3	P	
Tarumae summit cr.	Tr1	1999.07- 2000.08	Meteorol. Res. Inst. (2008)	310 (*3)	1.9×10^4	1.8×10^4	P	Estimation based on the GNSS repeat surveys (*3) Depth measured from the summit lava dome
	Tr2	2013.06.19- 2013.07.05	Koshiromaru (2014)	4200	3.4×10^5	5.3×10^6	U	Estimation based on the tilt and strain changes. The source location at ca. 1.5km north of the summit lava dome
Adatara Numano-Taira cr.	Ad	1998.07- 1999.06	Yamamoto *et al*. (2008)	60	4.8×10^3	5.2×10^3 (*12)	P	(*12) Converted by us from the volume change divided by the analyzed period
Azuma Ōana cr.	Az1	2003.09- 2004.11	Yoshida *et al*. (2012)	640 (*4)	1.5×10^5	1.3×10^5 (*5)	P	(*4) Converted by us into the depth from Ōana crater (1730m) (*5) Converted by us from the volume change divided by the analyzed period
	Az2	2006.05- 2007.05		270 (*4)	3×10^4	3×10^4 (*5)	P	
	Az3	2008.08- 2008.11		980 (*4)	7×10^4	2.8×10^5 (*5)	P	
	Az4	2014.10- 2015.01	Tohoku Univ. (2015)	3500	1.8×10^6	5.4×10^6 (*6)	U	Estimation using the continuous records of the JMA and the GSI (*6) Converted by us from the volume change divided by the analyzed period
Kusatsu-Shirane Yugama cr.	Ks	2014.03- 2015.11	Tokyo Inst. Tech. (2017)	540-840 (*7)	1.4×10^5	8.0×10^4	U	Estimation based on the tilt records at three sites (six components in total) (*7) Converted by us into the depth from Yugama crater (2040m)
Aso below Kusasenri	As1	2014.07.01- 2014.11.20		5000	6.8×10^5	1.7×10^6	M	Estimation based on the GNSS baseline changes, where the source position was assumed to be

	As2	2015.07.01-2015.09.13		5000	5.0×10^{5}	2.5×10^{6}	M	identical to the one obtained from the previous precise levelling surveys by Kyoto Univ. (Ohkura *et al*., 2009)
	As3	2016.07.01-2016.10.07		5000	5.5×10^{5}	2.0×10^{6}	M	
Kuchinoerabujima around Shindake or Furudake crs.	Kc1	1995.08/96.03- 2000.12	Iguchi *et al*. (2007)	600	1.7×10^{5}	3.4×10^{4}	P	Estimation based on the GNSS repeat surveys
	Kc2	2005.02-2006.01		300	2.4×10^{4}	2.6×10^{4}	P	
	Kc3	2006.01-2006.12/07.02		130	6.2×10^{3}	6.2×10^{3}	P	
	Kc4	2006.01-2014.04	Hotta and Iguchi (2017)	100	3.2×10^{4} (*8)	3.8×10^{3} (*9)	P	An FEM modelling based on the GNSS repeated surveys. Topography and layered rigidity taken into the modelling. (*8) Assumed an overpressure of 361MPa (*9) Converted by us from the volume change divided by the analyzed period
	Kc5a	2008.09-2009.02	Saito *et al*. (2015)	100		3.8×10^{3}	P	
	Kc5b	2008.09-2009.02		600		1.4×10^{4}	P	
	Kc6	2014.08-2015.03 (*10)	Yamamoto *et al*. (2017)	7500	2.6×10^{6}	4.5×10^{6} (*11)	M	Estimation based on two precise levelling surveys at the piedmont, in which the horizontal source position was fixed at Shindake crater (*10) The period after the eruption on August 3 in 2014 and before the re-eruption on May 29 in 2015 (*11) Converted by us from the volume change divided by the analyzed period